

SWI/SNF Complexes Containing Brahma or Brahma-Related Gene 1 Play Distinct Roles in Smooth Muscle Development^{∇†}

Min Zhang,¹ Meng Chen,¹ Ju-Ryoung Kim,¹ Jiliang Zhou,^{1‡} Rebekah E. Jones,¹ Johnathan D. Tune,¹
Ghassan S. Kassab,¹ Daniel Metzger,² Shawn Ahlfeld,³
Simon J. Conway,³ and B. Paul Herring^{1*}

Department of Cellular and Integrative Physiology, Indiana University School of Medicine, Indianapolis, Indiana 46202-5120¹;
Institute of Genetics and Molecular and Cellular Biology, Illkirch, CU de Strasbourg, France²; and *Wells Center for
Pediatric Research, Indiana University, Indianapolis, Indiana 46202³*

Received 22 November 2010/Returned for modification 20 December 2010/Accepted 8 April 2011

SWI/SNF ATP-dependent chromatin-remodeling complexes containing either Brahma-related gene 1 (Brg1) or Brahma (Brm) play important roles in mammalian development. In this study we examined the roles of Brg1 and Brm in smooth muscle development, *in vivo*, through generation and analysis of mice harboring a smooth muscle-specific knockout of Brg1 on wild-type and Brm null backgrounds. Knockout of Brg1 from smooth muscle in Brg1^{flox/flox} mice expressing Cre recombinase under the control of the smooth muscle myosin heavy-chain promoter resulted in cardiopulmonary defects, including patent ductus arteriosus, in 30 to 40% of the mice. Surviving knockout mice exhibited decreased expression of smooth muscle-specific contractile proteins in the gastrointestinal tract, impaired contractility, shortened intestines, disorganized smooth muscle cells, and an increase in apoptosis of intestinal smooth muscle cells. Although Brm knockout mice had normal intestinal structure and function, knockout of Brg1 on a Brm null background exacerbated the effects of knockout of Brg1 alone, resulting in an increase in neonatal lethality. These data show that Brg1 and Brm play critical roles in regulating development of smooth muscle and that Brg1 has specific functions within vascular and gastrointestinal smooth muscle that cannot be performed by Brm.

The SWI/SNF complex is perhaps the best-characterized mammalian ATP-dependent chromatin-remodeling complex (8). It is comprised of 7 to 11 components, which assemble into distinct complexes containing either Brahma-related gene 1 (Brg1) or Brahma (Brm) ATPase subunits. Brg1 and Brm are ubiquitously expressed in almost all tissues. Studies have suggested that Brg1 and Brm can have either redundant or distinct roles in regulating gene expression. For example, although Brg1 but not Brm has been shown to interact with Crp2 and subsequently induce expression of smooth muscle (SM)-specific genes (4), either Brg1 or Brm has been shown to be sufficient to support the smooth muscle myogenic activity of the myocardin family of activators in SW13 cells (33, 34). Data from knockout mice suggest that Brg1- and Brm-containing SWI/SNF complexes are functionally distinct *in vivo*. Brg1 knockout mice die early in embryonic development during the periimplantation stage (1), while global Brm knockout mice develop normally. On a 129/sv background but not a mixed 129/sv × C57BL/6 background, adult Brm knockout mice exhibited a higher body weight than wild-type (WT) littermates (24).

To circumvent the embryonic lethality observed in Brg1

knockout mice, several groups have generated and analyzed tissue-specific Brg1 knockout mice. These studies have revealed unique roles for Brg1-containing SWI/SNF complexes in development of many tissues (5, 11–13, 16, 20, 26). However, few of these studies have determined if Brm also contributes to these developmental pathways. One study combined a tissue-specific Brg1 knockout with a global Brm knockout to show that further loss of Brm did not exacerbate the erythropoietic or endothelial phenotypes of mice in which Brg1 knockout was driven by a Tie2-Cre transgene (12). Similarly, although Brg1 heterozygosity was shown to cause mammary tumors in a relatively small percentage of mice (~9%), when these mice were crossed to a Brm null background the prevalence of tumors did not increase (2). The Brm null, Brg1 heterozygous mice did, however, have a broader spectrum of tumors, with hemangiosarcomas being observed in addition to the mammary tumors. These data suggest that Brm is able to compensate for some of Brg1's functions. Haploinsufficiency of the SNF5 component of the SWI/SNF complex has also been associated with tumorigenesis *in vivo*, although loss of SNF5 resulted primarily in rhabdoid tumors (25). These data together with studies that have shown Brg1/Brm loss in many tumor cell lines and interactions of Brg1 and Brm with the Rb tumor suppressor suggest that the SWI/SNF complex likely plays an important role in tumorigenesis (21).

Several *in vitro* studies have suggested that SWI/SNF complexes play an important role in smooth muscle development (33, 34). Knockdown of either Brg1 or Brm attenuated expression of smooth muscle-specific contractile proteins in cultured smooth muscle cells (SMCs) (34). These data suggest that either there are nonoverlapping roles of Brg1 and Brm in

* Corresponding author. Mailing address: Department of Cellular and Integrative Physiology, Indiana University School of Medicine, 635 Barnhill Drive, Indianapolis, IN 46202-5120. Phone: (317) 278-1785. Fax: (317) 274-3318. E-mail: pherring@iupui.edu.

† Supplemental material for this article may be found at <http://mcb.asm.org/>.

‡ Present address: Center for Cardiovascular Sciences, Albany Medical College, Albany, NY.

∇ Published ahead of print on 25 April 2011.

SMCs or the combined total level of expression of Brg1 and Brm is required to maintain contractile protein expression in SMCs. To resolve this issue and to better determine the specific roles of Brg1 and Brm during development *in vivo*, we have generated mice that lack one or both alleles of Brg1 and/or Brm in smooth muscle cells and analyzed the resultant effects on development and function of smooth muscle-containing organs.

MATERIALS AND METHODS

Generation of knockout mice. All mouse experiments followed protocols approved by the Indiana University School of Medicine IACUC. Female Brg1^{lox/lox} mice (obtained from C.-P. Chang at Stanford) (16), were bred with male smMHC-Cre/eGFP mice (from Michael Kotlikoff at Cornell) (32) in order to generate a smooth muscle-specific knockout of Brg1. In smMHC-Cre/eGFP mice, Cre recombinase is expressed under the control of the smooth muscle-specific smMHC promoter (32). Mice were used on a mixed Sv129/C57B6 background. The male Brg1^{+/+} smMHC-Cre/eGFP^{-/+} mice were bred with female Brg1^{fl/fl} mice to generate smooth muscle-specific Brg1 knockout mice (Brg1^{fl/fl} smMHC-Cre^{-/+}) (smBrg1KO) (Fig. 1A and B). Because of a transient expression of Cre in the sperm of the Brg1^{fl/fl} smMHC-Cre^{-/+} mice (7), the floxed allele transmitted from these mice is recombined, resulting in a global heterozygous null allele of Brg1 in all tissues. There are thus four possible genotypes of the offspring: Brg1^{fl/fl} smMHC-Cre^{-/+} (SM-specific Brg1 knockout with global heterozygous Brg1 background; “smBrg1 knockout”), Brg1^{fl/fl} smMHC-Cre^{-/-} (global Brg1 heterozygous, which we use as a control for the knockout mice), Brg1^{fl/+} smMHC-Cre^{-/+} (SM-specific Brg1 heterozygous), and Brg1^{fl/+} smMHC-Cre^{-/-} (wild type). smBrg1/Brm double knockout mice were generated by crossing the Brg1^{fl/fl} mice and smMHC-Cre mice with Brm null mice as indicated in Fig. 1C. Brm null mice, originally generated by M. Yaniv's group (Pasteur Institute, Paris, France) (24), were obtained from Scott Bultman (University of North Carolina, Chapel Hill). Smooth muscle-specific Brg1 knockout mice with a Brm global heterozygous background were generated by crossing the male Brg1^{fl/+} smMHC-Cre^{-/+} mice with female Brg1^{fl/fl} Brm^{-/-} mice (Fig. 1D). Mouse genotyping was performed by standard procedures using the primers shown in Table S1 in the supplemental material.

Cre-dependent ROSA26-LacZ reporter mice. To examine Cre recombinase activity in the smMHC-Cre/eGFP mice, these mice were crossed with ROSA26^{loxstoplox}LAC (a Cre-dependent Lac reporter strain) mice. The reporter mice carry the LacZ reporter gene under the control of the ubiquitously expressed ROSA promoter sequences with an upstream STOP cassette flanked by lox sequences. In the presence of Cre recombinase activity, the STOP cassette is deleted and the LacZ gene is activated (Fig. 1E).

Tissue staining. β -Galactosidase staining, immunofluorescence, and hematoxylin-eosin (H&E) staining were performed as reported previously (28). For immunofluorescence analysis, the primary antibodies used were Brg1 (SC-17796 [Santa Cruz]; 1:100), SM1 and SM2 (15), telokin/myosin light-chain kinase (MLCK) (10), cleaved caspase 3 (Cell Signaling; 1:50), Ki67 (M7249 [Dako]; 1:25), and SM α -actin (Sigma; 1:500).

qRT-PCR. Quantitative reverse transcription-PCR (qRT-PCR) was performed as described previously, with the gene-specific primers shown in Table S2 in the supplemental material (33, 34).

Contractile measurements of isolated colon rings. The colon was carefully dissected and immediately washed in cold phosphate-buffered saline (PBS). Surrounding connective tissues and fat were gently removed, and the colon was cut into rings (1-cm axial length). The contractility of colon rings was measured as described previously for vascular rings (9, 18). Colon rings were mounted on L-shaped stainless steel supports, submerged in a 5-ml organ bath with Krebs buffer saturated with 95% O₂-5% CO₂, and held at 37°C. Krebs buffer contains 132 mM NaCl, 25 mM NaHCO₃, 5 mM KCl, 2.5 mM CaCl₂, 1.2 mM NaH₂PO₄, 1.2 mM MgCl₂, 0.025 mM EDTA, and 10 mM glucose, pH 7.4. A 2.5-g preload amount was empirically determined to result in the optimal length for most of the rings tested. To assess smooth muscle function, colon rings were contracted with 60 mM KCl or 0.1 μ M carbachol.

Contractile measurements of isolated whole colon. Colons were removed from neonatal mice and washed in cold PBS. Basal spontaneous contractility was measured using a video microscopy system as described previously (19). The diameter changes of the cannulated colon were observed under a video microscope and quantitated using dimensional analysis software (DIAMTRAK 3+; Australia).

Smooth muscle cell counting. SM2 (or telokin) and nuclear Hoechst immunofluorescent staining were performed on colon cryosections from smBrg1 knockout, Brm knockout, smBrg1/Brm double knockout, and littermate control mice. Nuclei of SM2 (or telokin)-positive cells in the circular smooth muscle layer were counted and normalized to the area of circular SM layer, which was measured using the software NIS-Elements AR 3.0 (Nikon).

RESULTS

Smooth muscle-specific knockout of Brg1. To generate mice harboring a deletion of Brg1 specifically in smooth muscle cells, we crossed the previously described Brg1 flox mice (27) with mice expressing Cre recombinase driven by the smooth muscle myosin heavy-chain promoter (Fig. 1) (32). To verify that the smMHC-Cre/eGFP transgene mediates appropriate smooth muscle-specific Cre recombinase activity, we crossed the smMHC-Cre/eGFP mice with ROSA26^{loxstoplox}LAC (a Cre-dependent Lac reporter strain) mice. Analysis of β -galactosidase activity in these mice shows that heterozygous Cre expression is sufficient to efficiently mediate recombination of the ROSA26 reporter allele specifically in smooth muscle tissues (Fig. 1E). A small amount of expression was also observed in the cardiac atria. To confirm that the transgene also mediates SM-specific recombination of the Brg1 locus, we extracted genomic DNA from smooth muscle-specific Brg1 heterozygous mice (Brg1^{fl/+} smMHC-Cre^{-/+}) and detected the recombined allele by PCR. The results showed that the Brg1 locus was recombined only in smooth muscle-containing tissues (bladder, colon, trachea, and aorta) and not in other tissues (colon epithelium, heart, skeletal muscle, liver, or kidney) (Fig. 1F). The relatively low level of recombination seen in the aorta may be partly due to a smaller smooth muscle cell contribution to the whole tissue. To verify that the recombined allele also resulted in loss of Brg1 protein, we analyzed expression of Brg1 protein in colon and aortic SMCs from smBrg1 knockout and littermate control mice using immunohistochemistry. There was abundant nuclear staining of Brg1 in colon smooth muscle cells in the control global heterozygous Brg1 animals (Brg1^{fl/fl} smMHC-Cre^{-/-}); however, in smBrg1 knockout mice (Brg1^{fl/fl} smMHC-Cre^{-/+}), little or no Brg1 staining was detected in SMCs (Fig. 2A). A similar loss of Brg1 was observed in aortic smooth muscle cells (Fig. 2B). The immunostaining for Brg1 is weaker in aortic smooth muscle than in colon smooth muscle as a result of the 4- to 5-fold-lower Brg1 expression in aorta than in colon (data not shown). The expression of Brg1 was also similarly decreased in the smooth muscle tissues from smBrg1/Brm double knockout mice (data not shown).

Neonatal lethality and pathologies in knockout mice. Analysis of the numbers of surviving smBrg1 knockout mice suggests that these mice exhibit a degree of neonatal mortality. Although smBrg1 knockout mice are detectable at the expected ratios at embryonic day 17.5 (E17.5), this ratio decreases by neonatal day 10 to 15.9% (expected progeny, 25%) (Table 1). This early neonatal lethality was due to cardiopulmonary defects. Analysis of 10 litters of newborn to 2-day-old mice (P0 to P2) revealed that approximately 33% of P0 to P2 smBrg1 knockout mice (6 out of 18) were cyanotic (darker blue skin color in Fig. 2C) and had dilated cardiac chambers consistent with left-to-right shunt and volume overload congestive heart failure. Isolated cyanotic heart/lungs failed to float in PBS compared to results for age-matched control littermates

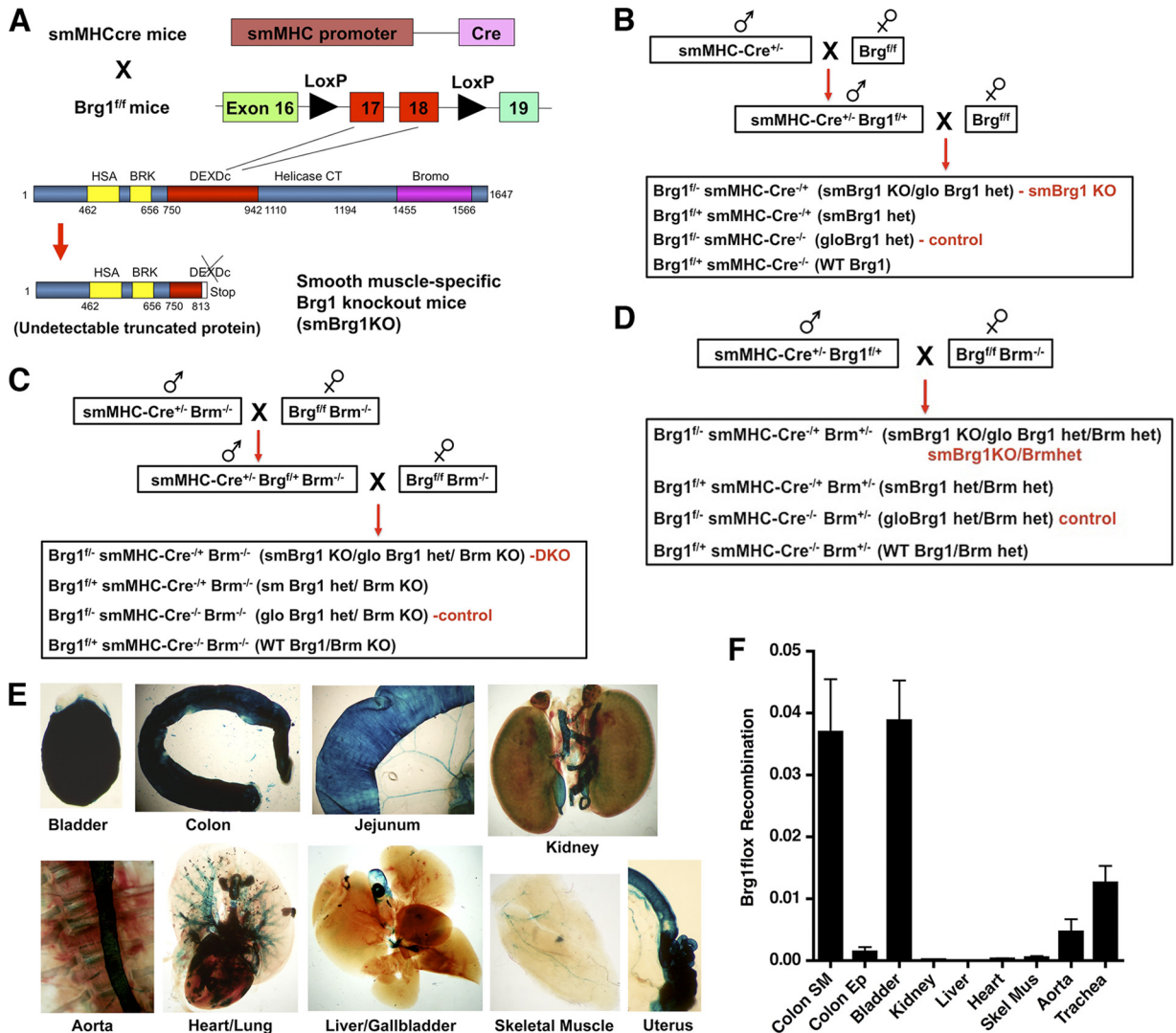


FIG. 1. Generation of smBrg1 knockout mice. (A) Exons 17 and 18 of Brg1, which are localized in the DEXDc domain, are flanked by two Loxp sites; after Cre-mediated recombination, an undetectable truncated Brg1 protein is translated. (B) Breeding scheme used to generate smooth muscle-specific Brg1 knockout mice (smBrg1 Brg1^{fl/-} smMHC-Cre^{+/-}) and global heterozygous Brg1 controls (Brg1^{fl/-} smMHC-Cre^{+/-}). (C) Breeding scheme used to generate smooth muscle-specific Brg1 knockout mice on a Brm null background (smBrg1/Brm smMHC-Cre^{+/-} Brg1^{fl/-} Brm^{-/-}). Littermate global Brg1 heterozygous/Brm null mice (smMHC-Cre^{+/-} Brg1^{fl/+} Brm^{-/-}) were used as controls. (D) Breeding scheme used to generate mice heterozygous for Brm on an smBrg1 background (smBrg1KO/BrmHet smMHC-Cre^{+/-} Brg1^{fl/+} Brm^{+/-}). Littermate global Brg1 and Brm heterozygous mice (smMHC-Cre^{+/-} Brg1^{fl/+} Brm^{+/-}) were used as controls. (E) β-Galactosidase activity is smooth muscle specific in smMHC-Cre^{+/-} ROSA26^{floxstopflox}LAC^{-/+} mice. Tissues from a neonatal mouse that was heterozygous for smMHC-Cre and ROSA26floxstopfloxLAC were dissected and stained for β-galactosidase activity using X-Gal (5-bromo-4-chloro-3-indolyl-β-D-galactopyranoside). Blue staining represents β-galactosidase-positive cells. (F) Smooth muscle-specific recombination of the Brg1 locus. Genomic DNA was extracted from tissues of smooth muscle-specific Brg1 heterozygous mice (Brg1^{fl/+} smMHC-Cre^{+/-}). Real-time PCR was performed using primers that amplify only the recombined Brg1 locus. Levels of the recombined Brg1 locus were normalized to a control single-copy gene (telokin) within the same sample in order to control for differences in DNA input. Data shown are relative quantities of recombined Brg1 locus after normalization to a loading control.

indicating that the lungs had failed to inflate ($n = 6/6$ cyanotic mutants examined). Additionally, although the lungs of smBrg1 knockout neonates were structurally normal, compared to control lungs they were hyperemic with accumulation of eosinophilic lipoproteinaceous material in the alveolar air space (Fig. 2D). Histology further revealed that cyanotic smBrg1 knockout neonates exhibit patent ductus arteriosus and ventricular septal defects (Fig. 2E). These pathologies were not, however, completely restricted to the smBrg1 knock-

out mice, as approximately 10% of P0 to P2 global heterozygous Brg1 mice (2 out of 19) were also cyanotic and exhibited patent ductus arteriosus and ventricular septal defects. In contrast, all of the noncyanotic smBrg1 knockout neonates examined exhibited normal closure of the ductus arteriosus (5/5). The smBrg1 knockout mice continue to display decreased survival as they age compared to global heterozygous or wild-type mice (Fig. 3A). In the absence of Brg1, deletion of one or both Brm alleles did not further alter the early neonatal mortality

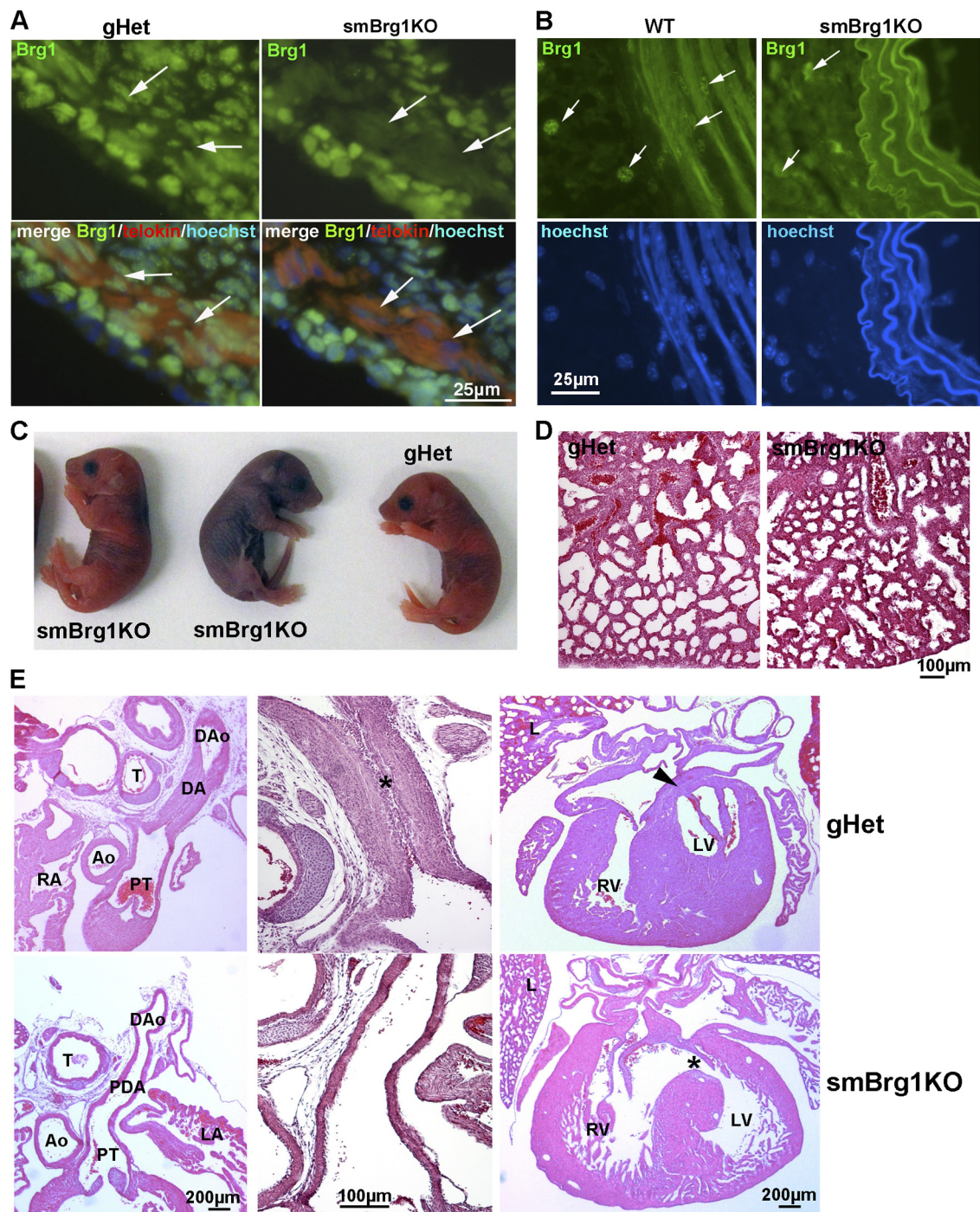


FIG. 2. Smooth muscle-specific knockout of Brg1 causes cardiovascular and pulmonary defects. (A) Immunofluorescent analysis of protein expression. Anti-Brg1-fluorescein isothiocyanate (FITC) (green), MLCK/telokin-rhodamine (red), and nuclear Hoechst (blue) immunofluorescence staining of colon cryosections from 2-day-old smBrg1 knockout ($Brg1^{fl-/-}$ smMHC-Cre $^{+/+}$) and littermate control ($Brg1^{fl-/-}$ smMHC-Cre $^{-/-}$) mice is shown. The smooth muscle layer is identified by the strong staining for MLCK/telokin. Arrows point to examples of cells within this smooth muscle layer. (B) Immunofluorescence staining of Brg1 (green) and nuclei (Hoechst) in aorta cryosections from 4- to 5-week-old smBrg1 knockout ($Brg1^{fl-/-}$ smMHC-Cre $^{+/+}$) and littermate wild-type ($Brg1^{fl+/+}$ smMHC-Cre $^{-/-}$) mice. (C) Images of newborn smBrg1 knockout and global heterozygous mice as indicated. The blue coloration in the middle mouse is indicative of poorly oxygenated blood. (D) H&E staining of the lung from a noncyanotic global Brg1 heterozygous mouse (gHet) and a cyanotic smBrg1 knockout mouse. (E) Patent ductus arteriosus (PDA) and interventricular septal defects (VSDs) in cyanotic smBrg1 knockout mice. Upper panels, transverse H&E-stained sections of torsos of global Brg1 heterozygous mice ($n = 3$) at postnatal day 1 showed expected normal closure of the ductus arteriosus (DA) in continuity within the descending aorta (DAo). At high power, intimal thickening in the form of proliferation of luminal endothelium and migration of medial smooth muscle cells was apparent in the DA (*). There is also the expected fused septum separating the left and right ventricles (arrowhead). Lower panels, transverse H&E-stained sections of torsos of smBrg1KO mice ($n = 4$) at postnatal day 1 showed patent ductus arteriosus (the PDA connects the main pulmonary artery to the descending aorta). At high power, DAs from smBrg1KO mice showed a single endothelial layer with an open lumen that was covered by a layer of normal intimal thickening. Additionally, there is also abnormal communication between left and right ventricles (*). Ao, aorta; PT, pulmonary trunk; RA, right atria; LA, left atria; T, trachea; RV, right ventricle; LV, left ventricle; L, lung.

TABLE 1. Percentages of surviving mice at E17.5, P1 to P10, and P21 to P28

Cross and genotype	% of surviving mice (mean \pm SEM) ^a		
	Embryo	P1–P10	3–4 wk
Brg1^{fl/fl} \times smMHC-Cre^{+/-} Brg1^{fl/+}			
Brg1 ^{fl/+} smMHC-Cre ^{-/-} (WT)	20.8 \pm 2.5	22.7 \pm 2.7	27.7 \pm 3.0
Brg1 ^{fl/+} smMHC-Cre ^{-/+} (smBrg1 heterozygous)	26.1 \pm 4.6	31.3 \pm 3.8	29.2 \pm 3.0
Brg1 ^{fl/-} smMHC-Cre ^{-/-} (global Brg1 heterozygous)	23.2 \pm 4.6	31.2 \pm 3.3	25.6 \pm 3.8
Brg1 ^{fl/-} smMHC-Cre ^{-/+} (smBrg1 KO/global Brg1 heterozygous)	29.9 \pm 5.1	15.9 \pm 2.3*	17.9 \pm 2.6*
Total no. of mice	87	222	278
Brg1^{fl/fl} Brm^{-/-} \times smMHC-Cre^{+/-} Brg1^{fl/+} Brm^{-/-}			
Brg1 ^{fl/+} smMHC-Cre ^{-/-} Brm ^{-/-} (Brm KO)	19.3 \pm 4.9	27.7 \pm 2.7	43.2 \pm 8.7
Brg1 ^{fl/+} smMHC-Cre ^{-/+} Brm ^{-/-} (smBrg1 heterozygous/Brm KO)	24.9 \pm 7.3	29.9 \pm 3.3	38.3 \pm 11.6
Brg1 ^{fl/-} smMHC-Cre ^{-/-} Brm ^{-/-} (global Brg1 heterozygous/Brm KO)	25.8 \pm 4.5	22.7 \pm 3.2	18.6 \pm 5.9
Brg1 ^{fl/-} smMHC-Cre ^{-/+} Brm ^{-/-} (smBrg1 KO/global Brg1 heterozygous/Brm KO)	30.1 \pm 6.3	18.1 \pm 2.6*	0
Total no. of mice	56	263	47
Brg1^{fl/fl} Brm^{-/-} \times smMHC-Cre^{+/-} Brg1^{fl/+}			
Brg1 ^{fl/+} smMHC-Cre ^{-/-} Brm ^{+/-} (WT Brg1/Brm heterozygous)		28.9 \pm 5.4	
Brg1 ^{fl/+} smMHC-Cre ^{-/+} Brm ^{+/-} (smBrg1 heterozygous/Brm heterozygous)		31.2 \pm 5.1	
Brg1 ^{fl/-} smMHC-Cre ^{-/-} Brm ^{+/-} (global Brg1 heterozygous/Brm heterozygous)		24.3 \pm 4.1	
Brg1 ^{fl/-} smMHC-Cre ^{-/+} Brm ^{+/-} (smBrg1 KO/global Brg1 heterozygous/Brm heterozygous)		15.7 \pm 3.1*	
Total no. of mice		109	

^a The mean percentage of mice, per litter, representing each of the indicated genotypes when genotyping was performed at E17.5, neonatal day P1 to P10, or 3 to 4 weeks after birth. The mice analyzed at 3 to 4 weeks are distinct from those genotyped at P1 to P10. *, significantly different from the expected 25% (1-sample *t* test).

rate (15.7% and 18.1%, respectively) (Table 1). Loss of both Brm alleles alone did not result in any significant neonatal lethality (data not shown). Similarly, in the absence of Brm, loss of a single Brg1 allele did not result in neonatal lethality (22.7%) (Table 1). These data suggest that a single Brg1 allele is sufficient to avoid the early neonatal lethality and that this lethality is a result of loss of Brg1, not Brm. In addition, the mortality is not a direct consequence of Cre overexpression, as Brg1^{fl/+} Cre^{-/+} mice (smooth muscle-specific heterozygote) were born with the expected frequencies and had survival indistinguishable from that of wild-type mice (Table 1 and Fig. 3A). Although deletion of both Brm alleles in the absence of Brg1 in SMCs does not alter the early neonatal mortality, this results in a marked increase in later neonatal mortality, with no mice surviving more than 2 weeks (Table 1). In the smBrg1 knockout mice, we observed enlarged intestine (colon, cecum, ileum, and jejunum) pathologies as the mice aged (more than 3 months) (Fig. 3B and C). The enlarged intestines appear to result from a dilatation and remodeling of the intestine rather than a thickening of the intestinal wall (Fig. 3C). Interestingly, although the Brg1 heterozygous/Brm knockout mice do not develop an enlarged intestine, all smBrg1 knockouts on a Brm heterozygous background develop megacolon and enlarged cecum and small intestine by about 4 weeks of age (Fig. 3D and E). All of the smBrg1/Brm double knockout mice also develop an enlarged gastrointestinal (GI) tract and urinary bladder prior to their death 7 to 10 days after their birth (Fig. 3F and G). The intestine in these mice was dilated and filled with air and fecal matter. These data demonstrate that the severity of the GI pathology is related to the number of Brg1 and Brm alleles lost. Although a single Brg1 allele is sufficient to avoid a GI pathology, a single Brm allele is not.

The intestine is shorter in smBrg1 knockout and smBrg1/Brm double knockout mice. Both the colon and small intestine were significantly shorter (by ~20%) in neonatal and adult, but

not embryonic, smBrg1 knockout mice than in control Brg1 heterozygous mice (Fig. 4A). In contrast, body weight, body length, and tibial length were not significantly different in smBrg1 knockout and Brg1 heterozygous control mice (Fig. 4B). In contrast, Brm knockout mice had unaltered intestinal length compared to wild-type mice (Fig. 4C). The intestinal pathology in smBrg1 knockout mice is further accentuated in mice lacking both Brg1 and Brm, such that the small intestine was also significantly shorter (20%) in mice at embryonic day 17.5 (Fig. 4D). Mice lacking Brg1 and heterozygous for Brm (smBrg1KO BrmHet) also exhibited shorter colons and small intestines than Brg1/Brm double heterozygous mice (Fig. 4E).

Colons from smBrg1 knockout and smBrg1/Brm double knockout mice exhibit impaired contractility. Isolated colonic rings from adult (2- to 3-month-old) smBrg1 knockout mice stimulated to contract with either 60 mM KCl or 0.1 μ M carbachol exhibited a marked impairment of force production compared to rings obtained from littermate Brg1 heterozygous control mice (Fig. 5A). Using the same method, we observed no differences in the contractility of colons from adult Brm knockout mice and from littermate wild-type control mice (Fig. 5B). Since smBrg1/Brm double knockout mice die as neonates, we were unable to measure contractility of colonic rings using our myograph system. Instead we measured the contractility of cannulated colonic segments from mice at neonatal day 5 to 7 using a video microscopy system. This analysis revealed that the normal basal spontaneous contractile activity of control colon (Brg1^{fl/-} Brm^{-/-} smMHC-Cre^{-/-}) was completely absent in colons from smBrg1/Brm double knockout mice (see Movies S1 and S2 in the supplemental material). To further quantitate these changes, the diameters of the colons from control (Brg1^{fl/-} Brm^{-/-} smMHC-Cre^{-/-}) and smBrg1/Brm double knockout (Brg1^{fl/-} Brm^{-/-} smMHC-Cre^{+/-}) mice were recorded over time, and a representative plot is shown in Fig. 5C. The increases and decreases of diameter of the colon

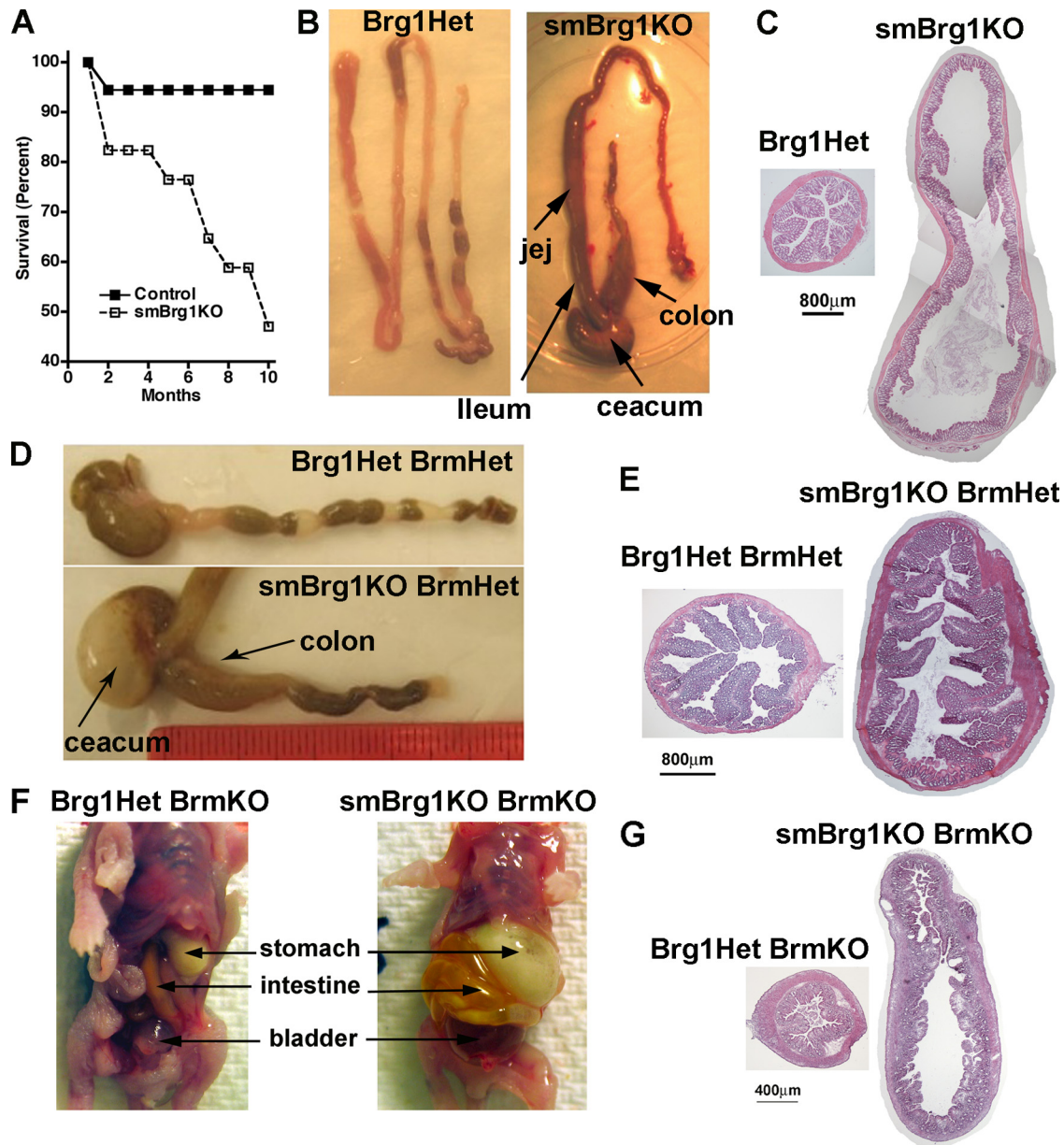


FIG. 3. GI pathologies in knockout mice. (A) Postnatal mortality in smBrg1 knockout mice. Of 17 smBrg1KO mice that were alive at 1 month of age, only approximately 50% survived to 10 months of age, compared to 95% of control mice (36 mice, including a mix of gloBrg1Het, smBrg1Het, and WT mice). (B) Some smBrg1 knockout mice develop enlarged colon, cecum, ileum, and jejunum after 4 to 6 months. (C) H&E staining of cross sections of proximal colon from a 6-month-old smBrg1 knockout mouse exhibiting megacolon and a Brg1 heterozygous littermate control mouse. (D) All smBrg1KO/Brm heterozygous mice ($Brg1^{fl/fl}$ smMHC-Cre^{+/-} Brm^{+/-}) developed enlarged intestines after 1 month. (E) H&E staining of cross sections of proximal colon from 1-month-old smBrg1KO/Brm heterozygous mice and littermate Brg1/Brm heterozygous control mice. (F) Stomach, intestine, and bladder were dilated in all neonatal smBrg1/Brm double knockout mice (the example shown is from neonatal day 7). (G) H&E staining of cross sections of proximal colon from smBrg1/Brm double knockout ($Brg1^{fl/fl}$ smMHC-Cre^{+/-} Brm^{-/-}) and control Brg1Het/Brm knockout ($Brg1^{fl/fl}$ smMHC-Cre^{-/-} Brm^{-/-}) mice.

correlate to the relaxation and contraction of the circular smooth muscle layer, respectively. In colons from control mice, diameters spontaneously changed from 2.1 mm to 1.8 mm (Fig. 5C, left panel), while the diameters of colons from double knockout mice remained constant at 2.4 mm (Fig. 5C, right panel).

Contractile protein expression is attenuated in smBrg1 knockout and smBrg1/Brm double knockout mice. We utilized

real time RT-PCR analysis of mRNA expression and Western blotting to evaluate the expression of smooth muscle-specific contractile proteins in smBrg1 knockout, Brm null, and smBrg1/Brm double knockout mice. In the smBrg1 knockout mice, we detected a small but significant decrease in the mRNAs encoding many smooth muscle-specific contractile proteins (Fig. 6A). In contrast, there was no change in expression of serum response factor (SRF)-dependent early response

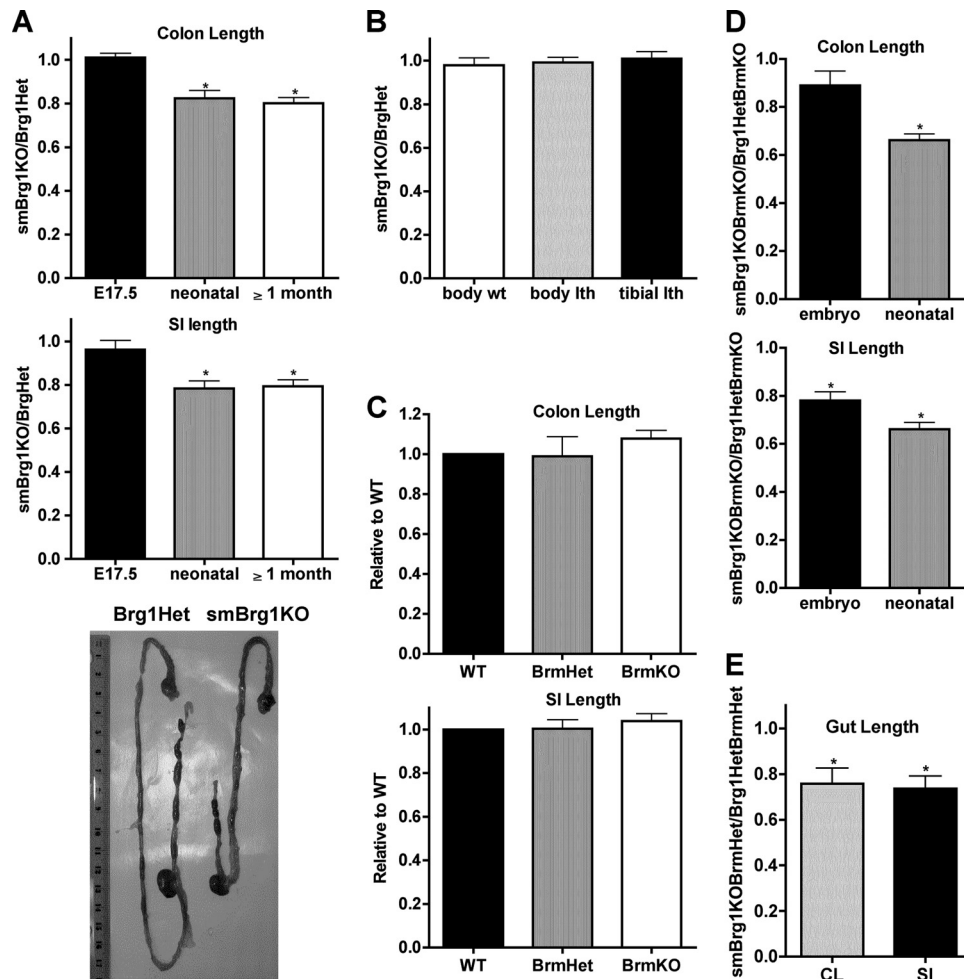


FIG. 4. The intestines of smBrg1 knockout and smBrg1/Brm double knockout mice are shorter than those of littermate controls. (A) The colons and small intestines (SI) of embryonic, neonatal, and adult smBrg1 knockout mice were measured, and lengths are expressed relative to the length of intestine in control (Brg1Het) mice (set to 1) as indicated. The lower panel is a representative picture of the whole gut from neonatal smBrg1 knockout and global heterozygous Brg1 littermate mice. (B) Body weights, body lengths, and tibial lengths of smBrg1 knockout mice were compared to those of littermate heterozygous Brg1 littermate mice ($n = 4$ or 5). (C to E) The colons (CL) and small intestines of neonatal (C and E) or neonatal and embryonic (D) knockout mice were measured, and lengths are expressed relative to the length of intestine in control mice (set to 1) as indicated. Data shown are the means \pm standard errors of the means (SEM) from 5 to 7 mice. *, $P < 0.05$.

genes (c-fos and SRF), SRF coactivators (myocardin and MRTFA), or several other reported Brg1 target genes (adamts1, laminin1, wnt4, wnt5a, c-myc, axin2, cyclinD1, and p21) or of the voltage-gated calcium channel (Cav1.2). We did not observe any significant differences in expression of contractile proteins or their mRNAs in colons (Fig. 6B and D) and bladders (data not shown) from neonatal Brm null mice compared to wild-type littermates. In contrast to previous reports for other tissues (24), we did not observe any compensatory changes in expression of Brg1 in the colons (Fig. 6D) or bladders (data not shown) of Brm knockout mice. In smBrg1/Brm double knockout mice there was attenuated expression of smooth muscle-specific contractile protein mRNAs similar to that seen in the smBrg1 knockout mice (Fig. 6C). In the smBrg1/Brm double knockout mice we also detected a significant decrease in the expression of several contractile proteins, including telokin, smMLCK, SM1, SM α -actin, and SM22 α by

Western blotting (a representative blot and quantitation of data obtained from several mice are shown in Fig. 6E and F).

SMCs in the colons of smBrg1 knockout and smBrg1/Brm double knockout mice are disorganized. Histological staining of colon sections from neonatal smBrg1 knockout (Fig. 7A) and smBrg1/Brm double knockout (Fig. 7B) mice revealed a disorganization of the circular smooth muscle layer in the knockout mice. The SMCs were not aligned as evenly as those of control mice and appear to have lost the typical spindle shape of normal SMCs, whereas SMCs in the colons of Brm knockout mice appeared normal (data not shown). Electron micrograph analysis further revealed ruffled borders and highly invaginated margins of the circular SMCs, with more space (a less electron-dense region) between these cells in colons from adult smBrg1 knockout mice compared to the very straight and parallel borders of the smooth muscle cells from the Brg1 heterozygous control mice (Fig. 7C).

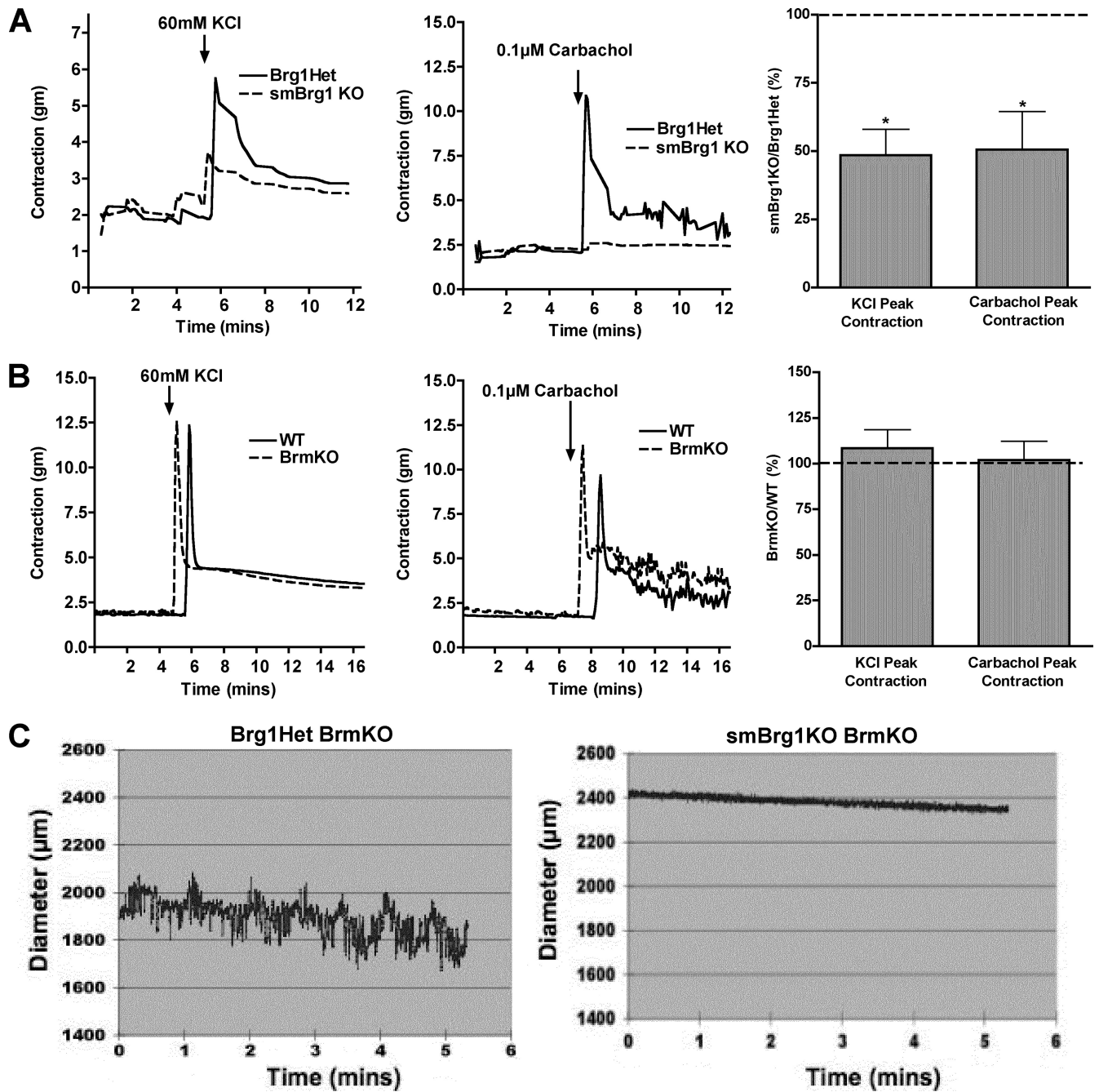


FIG. 5. The contractility of the colons from smBrg1 knockout and smBrg1/Brm double knockout mice is impaired. (A and B). Colons from adult mice (2 to 3 months old) were cut into 0.5-cm-long rings. The rings were hung in a myograph and contractility in response to KCl or the muscarinic agonist carbachol measured. Representative traces are shown together with average data obtained from 4 or 5 different mice. (A) Data obtained from smBrg1 knockout mice. (B) Data obtained from Brm knockout mice. The recordings have been offset slightly to allow both WT and KO tracings to be better visualized. (C) Representative recording of the spontaneous diameter changes seen in the colons from smBrg1/Brm double knockout mice and Brg1Het/Brm KO controls (7 days old). A dynamic view of these changes can be seen in Movies S1 and S2 in the supplemental material.

smBrg1 and smBrg1/Brm double knockout mice have increased smooth muscle cell apoptosis. In addition to regulating differentiation, Brg1 regulates apoptosis and proliferation in some cell types (22, 27, 29). We thus hypothesized that the shorter gut observed in Brg1 knockout mice may result from increased SMC apoptosis and/or decreased proliferation of

SMCs. To evaluate apoptosis, we performed immunofluorescent staining of cleaved caspase 3 on sections of proximal and distal colon obtained from embryonic and neonatal smBrg1 knockout mice or smBrg1/Brm double knockout mice (Fig. 8A). In E17.5 embryos from either smBrg1 knockout or smBrg1/Brm double knockout mice, there was no detectable

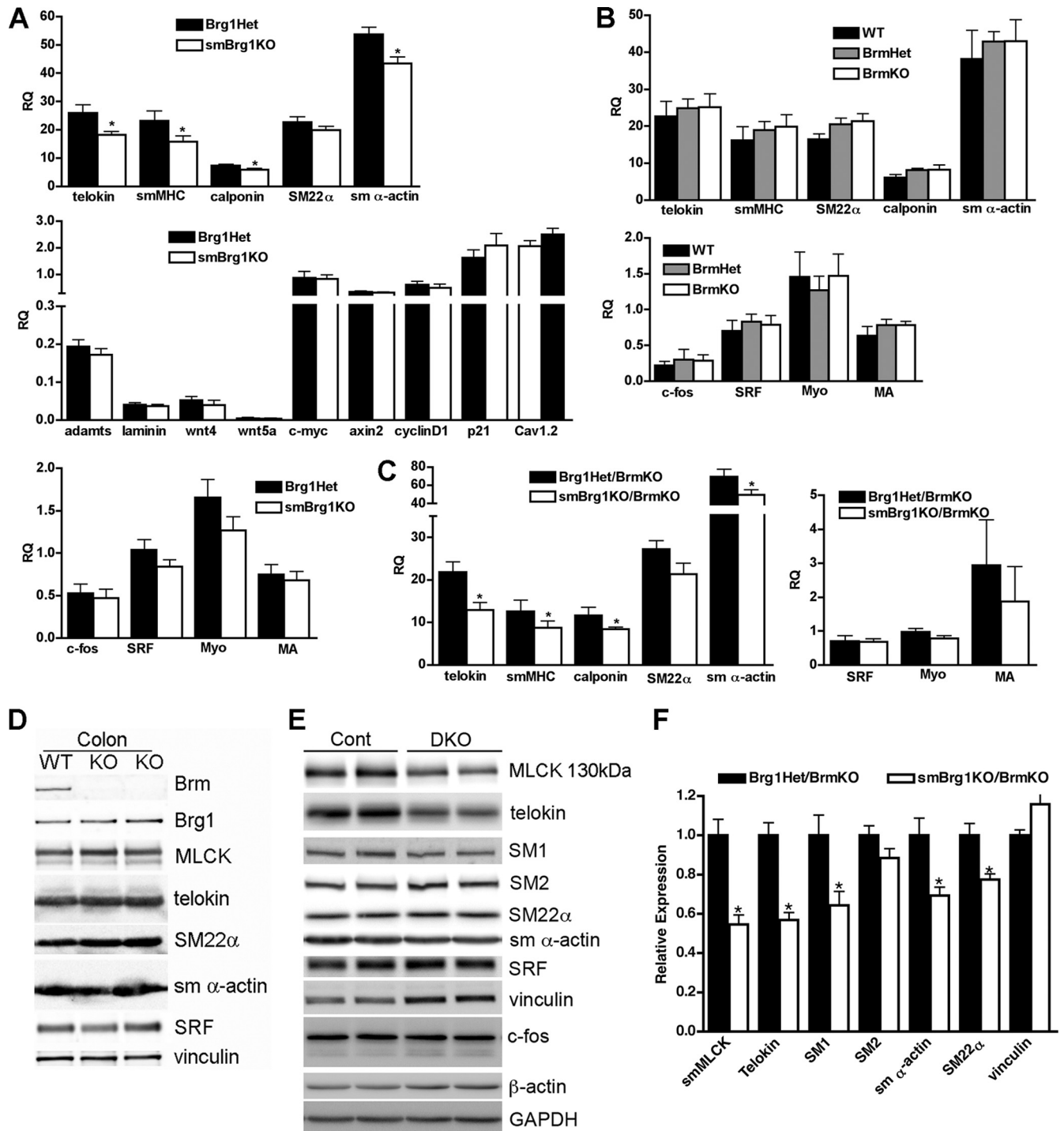


FIG. 6. Expression of contractile proteins is decreased in smBrg1 knockout and Brg1/Brm double knockout mice but not in Brm knockout mice. (A) RNA was extracted from colons of neonatal smBrg1 knockout and global Brg1 heterozygous controls and mRNA expression quantitated by real-time qRT-PCR. Transcript levels were normalized to a hypoxanthine phosphoribosyltransferase (HPRT) internal loading control, and relative expression levels (RQ) are shown (relative expression = $2^{-\Delta C_T}$, where $\Delta C_T = C_{T\text{experimental}} - C_{T\text{HPRT}}$). Each bar represents the mean \pm SEM for samples obtained from 9 mice. (B) qRT-PCR analysis of mRNA extracted from colons of neonatal Brm knockout, Brm heterozygous, and WT control mice. Data presented are the mean \pm SEM relative expression (RQ) of samples obtained from 5 or 6 mice. Myo, myocardin; MA, MRTFA. (C) qRT-PCR analysis of mRNA obtained from colons of 6 to 8 neonatal smBrg1/Brm double knockout (DKO) and littermate global Brg1Het/Brm knockout (Cont) mice. For all qRT-PCR data, statistical significance was determined using SPSS mixed-models linear test analysis. *, $P \leq 0.05$. (D and E) Western blot analysis of protein expression from two Brm knockout mice and one wild-type mouse (D) and from two smBrg1/Brm double knockout mice (DKO) and littermate Brg1Het/Brm knockout control mice (Cont) (E). (F) Quantitation of protein expression in smBrg1/Brm double knockout mice. Means \pm SEM are shown; $n = 3$ to 4. *, $P < 0.05$ as determined by Student's t test.

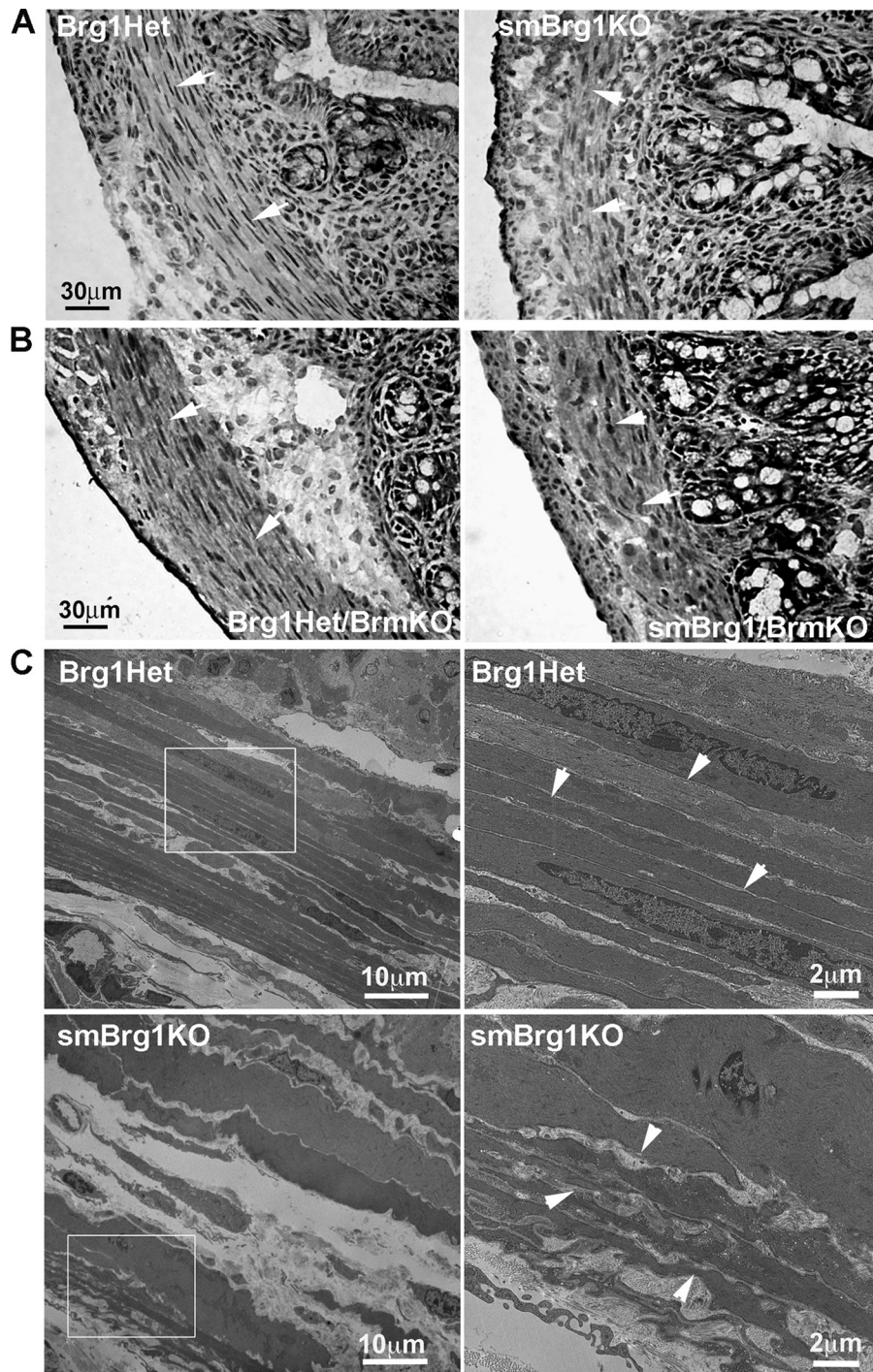


FIG. 7. Smooth muscle cells in the circular smooth muscle layer of colons from smBrg1 knockout and smBrg1/Brm double knockout mice are disorganized. (A and B) Ultrastructure analysis, using H&E staining, of neonatal smBrg1 knockout mice and littermate global Brg1 heterozygous controls (A) and neonatal smBrg1/Brm double knockout mice and global Brg1 het/Brm knockout controls (B). Arrowheads point to cells within the circular smooth muscle layer. (C) Electron micrographs of colons from 3-month-old smBrg1 knockout mice and littermate global Brg1 heterozygous controls. Boxed areas in the left panels are magnified in the right panels. Arrowheads point to the cell borders.

cleaved caspase 3 in the smooth muscle layer of the colon (data not shown). In neonatal knockout mice, we observed more apoptotic cells in each cross section from smBrg1 knockout and smBrg1/Brm double knockout mice than in those from controls (2.5 and 5.2 cells per section compared to 0.38 and

0.67 cells per section, respectively) (Fig. 8A and B). In neonatal Brm knockout mice, there were no differences in the numbers of active caspase 3-positive cells compared to those in WT controls (Fig. 8B). To examine possible changes in SMC proliferation, we performed immunofluorescent staining for the

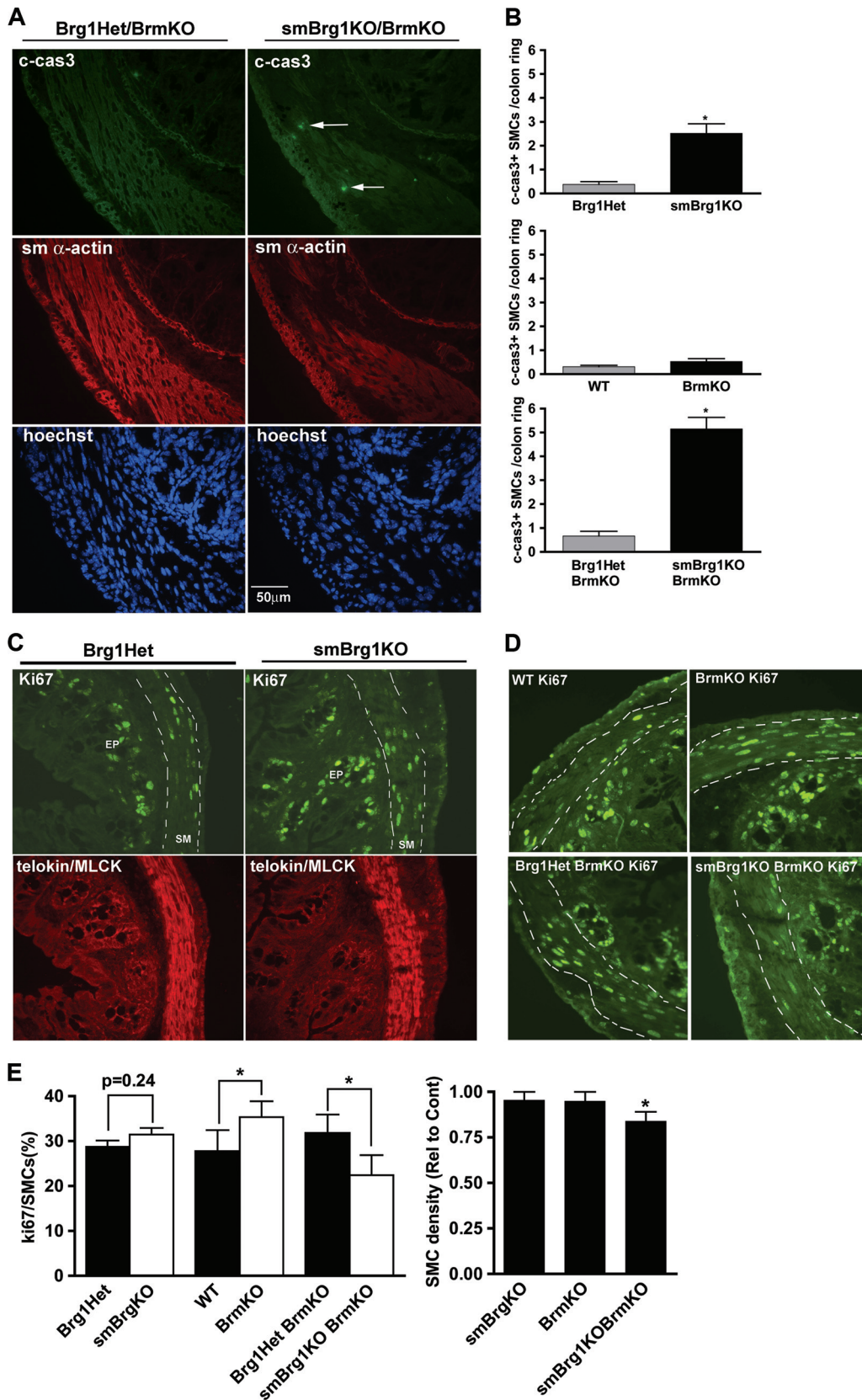


FIG. 8. Alterations in apoptosis and proliferation in colon smooth muscle from knockout mice. (A) Cleaved caspase 3 (green), SM α -actin (red), and Hoechst nuclear (blue) staining of colons from neonatal smBrg1/Brm double knockout and control Brg1Het/Brm knockout mice. Arrows point to cleaved caspase 3-positive SMCs. (B) Cleaved caspase 3-positive SMCs in the circular muscle layer of colons from knockout mice

proliferation marker Ki67. In the colons from 3-month-old smBrg1 knockout and control mice, Ki67-positive cells were found in the crypt epithelium above the submucosa layer but not in SMCs as reported previously (data not shown) (23). However, in the colons from neonatal mice, Ki67-positive cells were found in both the epithelium and smooth muscle layer (Fig. 8C and D). Surprisingly, the number of Ki67-positive SMCs in smBrg1 knockout mice was not significantly different from that in Brg1 heterozygous controls (Fig. 8E). Similar results were observed at E17.5 (data not shown). Consistent with previous reports of increased proliferation in Brm knockout mice (24), we observed more Ki67-positive SMCs in the colonic circular smooth muscle layer from neonatal Brm knockout mice than in that from littermate WT control mice (Fig. 8D and E). In contrast, in smBrg1/Brm double knockout mice we found significantly fewer Ki67-positive SMCs in the colonic circular smooth muscle layer than in that from littermate smBrg1 heterozygous/Brm knockout control mice (Fig. 8D and E), while there was no difference in E17.5 mice (data not shown). It should be noted, however, that these control mice are Brm null and hence have elevated proliferation compared to wild-type mice. The decreased proliferation observed in the neonatal smBrg1/Brm double knockout mice thus simply returned their proliferation rate back to that of wild-type mice. The smooth muscle cell density was also not changed in neonatal smBrg1 knockout or Brm knockout mice but was decreased in neonatal smBrg1/Brm double knockout mice (Fig. 8E).

DISCUSSION

Our data demonstrate that Brg1 and Brm play critical roles in regulating the development and physiology of gastrointestinal (GI) smooth muscle and that Brg1 has specific functions within GI smooth muscle that cannot be performed by Brm. Similarly, we found that Brg1 also has specific functions in the vascular system, where it is important for closure of the ductus arteriosus. Knockout of Brg1 from GI smooth muscle resulted in decreased expression of smooth muscle-specific contractile proteins (Fig. 6), impaired contractility (Fig. 5), shortened intestines (Fig. 4), disorganized SMCs (Fig. 7), and a small increase in apoptosis of intestinal SMCs (Fig. 8). Although knockout of Brm alone did not alter any of these parameters, knockout of Brg1 and Brm together accentuated the effects of knockout of Brg1 alone, resulting in a slightly greater decrease in expression of each contractile protein and intestinal length and a slightly greater increase in apoptosis (Fig. 4, 6, and 8). The double knockout of Brg1 and Brm resulted in a more marked decrease in GI motility and a dramatic increase in late neonatal lethality compared to knockout of Brg1 or Brm alone (Fig. 5; Table 1). The severity of the GI phenotype in the

mice correlates with the total number of Brg1 and Brm alleles but with the loss of Brg1 alleles being more imperative. Mice with no Brg1 or Brm were most severely affected; they developed enlarged intestines and died within 2 weeks after birth. Most mice with a single Brm allele and no Brg1 alleles developed megacolon/megaintestine by about 4 weeks of age, whereas mice with both Brm alleles but no Brg1 alleles were less affected and developed megacolon/megaintestine at a lower frequency and at a more advanced age. Mice with both Brg1 alleles but no Brm alleles were least affected and did not develop an obvious intestinal pathology. It is likely that the combined effects of decreased contractile protein expression and disorganization of the SMCs are major contributors to the attenuated contractility seen in the smBrg1 and smBrg1/Brm knockout mice. As high-KCl-induced depolarization stimulates contraction primarily through opening voltage-gated calcium channels, we examined expression of these channels in the smBrg1 knockout mice and found that their expression was not altered in the knockout mice (Fig. 6A). However, this does not rule out the possibility that changes in the expression of other calcium regulatory or contractile regulatory proteins could be additionally contributing to this phenotype. In the smBrg1 knockout mice the contractility defects can be detected prior to the development of the overt intestinal pathology, suggesting that the attenuated contractility causes motility defects that result in enlarged intestines due to their inability to appropriately move and expel feces. It is not clear if the small differences in contractile protein expression or smooth muscle disorganization in the smBrg1/Brm double knockout mice compared to the smBrg1 single knockout mice are sufficient to explain the dramatic differences in contractility and late neonatal morbidity of these two groups of mice. Similarly, it does not appear that the small changes in proliferation could account for these differences. Although we did observe an increase in apoptosis in the neonatal smBrg1/Brm double knockout mice compared to the smBrg1 single knockout mice, this was not evident at E17.5. It is thus likely that this increase is a consequence rather a cause of the pathology. It remains possible that changes in expression of currently unidentified proteins may be contributing to the pathological and motility differences observed between smBrg1 knockout and smBrg1/Brm double knockout mice.

In this study we have focused primarily on the intestinal pathology in the smBrg1 and Brm knockout mice, partly because this is the most obvious pathology exhibited by these mice. This pathology also likely accounts for the majority of the mortality of the smBrg1/Brm double knockout mice seen at about 10 days after birth. As our knockout mice will have Brg1 deleted from most smooth muscle tissues, it is likely that other smooth muscle-containing organs also exhibit some defects. In support of this, we observed greatly enlarged bladders in the

were counted and quantitated. Significant differences between knockout and control mice were determined by Student's *t* test. *, $P \leq 0.05$. Data are the means \pm SEM from 3 to 5 mice. (C and D) Ki67 (green) and telokin/MLCK (red) immunofluorescent staining of colon from neonatal smBrg1 knockout (C) and Brm knockout and smBrg1/Brm double knockout (D) mice. (E) Left panel, Ki67-positive SMCs were quantitated in stained sections similar to those shown in panels C and D except that nuclei were also stained with Hoechst stain. Right panel, smooth muscle cell density in the circular muscle layer of colons from knockout mice expressed relative to the appropriate control mice (indicated in panels C and D). Data are the means \pm SEM from 5 or 6 mice. *, $P \leq 0.05$.

smBrg1/Brm double knockout mice (Fig. 3F), suggestive of contractility defects in the bladder smooth muscle. We also observed decreased expression of contractile protein expression in the bladder tissue from smBrg1/Brm double knockout mice (data not shown). However, the early neonatal lethality seen in some of the smBrg1 knockout mice cannot be easily explained by defects in GI or bladder motility, as intestinal defects manifest typically several days after birth (Table 1) and the elevated mortality in these mice occurs neonatally in the first day or two after birth. This time period would more likely suggest cardiopulmonary abnormalities (6). In support of this, we could detect a loss of Brg1 in vascular smooth muscle (Fig. 2B), and about 33% (6 out of 18) of newborn smBrg1 knockout mice were cyanotic and exhibited the cardiac outflow tract defect, patent ductus arteriosus, and obligatory associated ventricular septal defects (Fig. 2E). The ductus arteriosus is a transient *in utero* vessel connected to the descending aorta, which allows 90% of the fetal circulation ejected from the right ventricle to bypass the immature developing lungs. Normally the muscular wall of the ductus arteriosus constricts at birth, coincident with aeration of the lungs and closure of the foramen ovale shunt. It is, however, not completely clear if these defects are solely due to Brg1 knockout from vascular smooth muscle cells within the ductus arteriosus, as we also observed similar cardiopulmonary defects in 10% (2 out of 19) of global Brg1 heterozygous mice. Knockout of Brg1 in cardiac muscle and embryonic smooth muscle using an SM22 α Cre transgene has been reported to result in thin ventricles and ventricular septation defects (13). Although no defects in outflow tract formation were reported in these mice, as the mice died around E12.5, outflow tract-remodeling defects such as patent ductus arteriosus would not be evident at this stage. The lack of effects on the ventricular muscle thickness in the smBrg1 knockout mice further argues that the defects observed in these mice are not likely caused by ectopic Cre expression in the ventricles. Together these data suggest that Brg1 likely regulates genes in vascular smooth muscle cells that mediate the morphological changes required for closure of the ductus arteriosus.

In addition to patent ductus arteriosus, the lungs of the cyanotic smBrg1 knockout mice demonstrated overwhelming atelectasis compared to those of littermate controls. Areas of lung that were aerated had hyperemic septae, and an eosinophilic transudate lined the airspaces. While these findings may be partially explained by the persistence of the ductus arteriosus with resultant pulmonary vascular bed overflow, they are also consistent with surfactant deficiency. Surfactant is composed of phospholipids and proteins and is secreted by alveolar type II epithelial cells to coat the airspace, reduce surface tension, and facilitate expansion of the lungs. Surfactant protein B (SP-B) is vital to the surface tension-reducing properties of surfactant (30), and its deficiency causes neonatal lethality and diffuse lung disease characterized by atelectasis and accumulation of dense lipoproteinaceous material in the alveolar airspaces (31). Brg1 has been shown to facilitate binding of the transcription factor Nkx2-1 to the promoter region of the surfactant protein B gene (*Sftpb*) and enhance production of SP-B by alveolar epithelial cells (3). Loss of Brg1 in this cell culture model resulted in decreased production of SP-B. While this has not yet been confirmed *in vivo*, it may partially explain

why systemic loss of a single copy of Brg1 in our model was associated with pulmonary findings consistent with surfactant deficiency and neonatal death.

The decreased expression of contractile proteins seen in the smBrg1 and smBrg1/Brm knockout mice is consistent with our previous *in vitro* data which showed that small interfering RNA (siRNA)-mediated knockdown of either Brg1 or Brm in cultured vascular smooth muscle cells decreased expression of SRF-dependent contractile proteins (34). Similarly, expression of dominant negative Brg1 attenuated expression of contractile proteins in colonic smooth muscle cells (33). As we did not observe any significant change in SMC density, it is likely that per unit length of intestine the decreased expression of smooth muscle contractile proteins is not due to a decreased number of smooth muscle cells. The relatively small changes in expression of contractile proteins seen in the smBrg1 and smBrg1/Brm knockout mice may reflect the timing of Cre expression in these mice. As Cre is driven by the smooth muscle myosin heavy-chain promoter, a relatively late marker of differentiated smooth muscle cells, Cre will be expressed only once smooth muscle cells have already differentiated. The modest changes in contractile proteins seen in the knockout mice may thus reflect the greater need for SWI/SNF activity during, rather than after, differentiation. These data are consistent with the previous *in vitro* cell culture studies in which the smooth muscle cells remained proliferating and were not fully differentiated, thus explaining their greater dependence on ongoing SWI/SNF-mediated chromatin remodeling. This model is also consistent with the observations that the myocardin family of SRF coactivators require either Brg1 or Brm to facilitate SRF binding and subsequent induction of smooth muscle-specific genes (33, 34). We propose that once these genes are active and SRF is bound, continued chromatin remodeling may not be as important for maintaining expression of the contractile proteins in relatively quiescent differentiated smooth muscle cells.

The decreased intestinal length in smBrg1 knockout mice and smBrg1/Brm double knockout mice, but not Brm knockout mice, suggests that this phenotype is likely a primary consequence of the loss of Brg1-containing SWI/SNF complexes. The shorter gut in smBrg1 and smBrg1/Brm knockout mice is unlikely to be a result only of decreased SMC proliferation or increased apoptosis. Proliferation was not significantly altered in these mice (Fig. 8C to E), and the increase in apoptosis was fairly small (Fig. 8A and B). Although Brg1 has been reported to affect the cell cycle in some cells, (14, 17), our data suggest that this effect is cell type specific, reflecting different functions of Brg1 in different types of tissues and cells. The change in intestinal length was apparent in smBrg1/Brm double knockout mice at E17.5, before a significant change in apoptosis was observed (Fig. 4 and data not shown). We thus favor the hypothesis that the misorganization of the smooth muscle within the intestine is a major factor contributing to the decreased intestinal length. As SMCs were disorganized in the intestines of Brg1 and Brg1/Brm knockout mice (Fig. 7) but not in those of Brm knockout mice (data not shown), this would suggest that this disorganization is primarily a result of the loss of Brg1-containing SWI/SNF complexes. Although decreased contractile protein expression could contribute to the disorganization of intestinal smooth muscle cells, through disrupting the cytoskeletal architecture, it is likely that altered

expression of other Brg1 target genes also contributes to this pathology. As changes in cell-cell and cell-matrix interactions could be reasonably proposed to affect this phenotype, we initially screened a number of extracellular matrix and adhesion molecules using a PCR array (SA Biosciences) and attempted to validate potential targets by qRT-PCR. These experiments, however, did not identify any significant changes in the genes examined (such as Col1a1, Col5a1, emilin1, Icam1, Itgam, Mmp3, Sparc, adamts1, and laminin1) (Fig. 6A and data not shown). Similarly we did not observe any changes in expression of proteins that have previously been linked to regulation of intestinal length (wnt4, wnt5a, c-myc, axin2, cyclinD1, p21, BMP4, Gli1, and Gli2) (Fig. 6A and data not shown). To better identify the Brg1-specific target genes that could be contributing to the intestinal pathology, future studies will need to utilize a whole-genome-wide array to analyze gene expression in pure populations of SMCs isolated from Brg1 knockout mice.

In conclusion, our study illustrates new and important roles of Brg1 and Brm in smooth muscle development. We provide evidence that although Brg1 has some unique roles in gastrointestinal development, both Brg1 and Brm cooperate to mediate the physiological development and function of the GI tract. The GI pathologies observed in the smBrg1 knockout mice are reminiscent of clinical conditions that result in visceral myopathies of unknown cause. Inherited mutations that abrogate Brg1 expression or function cannot cause these clinical conditions, as they would be incompatible with early fetal development. However, our findings suggest the intriguing possibility that alterations in signaling pathways that modulate SWI/SNF function to cause epigenetic changes in chromatin structure could play a role in the etiology of these diseases. Alternatively, mutations in specific SWI/SNF target genes could be the cause of idiopathic intestinal myopathies. Additional studies will be needed to address these exciting possibilities.

ACKNOWLEDGMENTS

We thank C.-P. Chang, Michael Kotlikoff, and Scot Bultman for providing mice used in this study, Xiao Lu for help with contractility measurements, and Liang Chen and Mingsheng Wang for help with tissue processing.

This research was supported in part by NIH grant DK61130 to B.P.H. and Riley Children's Foundation, the Indiana University Department of Pediatrics (Neonatal-Perinatal Medicine), and NIH grant HL60714 to S.J.C. M.Z. was supported by a fellowship from AHA and J.Z. by an AHA Scientific Development Grant.

REFERENCES

- Bultman, S., et al. 2000. A Brg1 null mutation in the mouse reveals functional differences among mammalian SWI/SNF complexes. *Mol. Cell* **6**:1287–1295.
- Bultman, S. J., et al. 2008. Characterization of mammary tumors from Brg1 heterozygous mice. *Oncogene* **27**:460–468.
- Cao, Y., et al. 2010. Epigenetic mechanisms modulate thyroid transcription factor 1-mediated transcription of the surfactant protein B gene. *J. Biol. Chem.* **285**:2152–2164.
- Chang, D. F., N. S. Belaguli, J. Chang, and R. J. Schwartz. 2007. LIM-only protein, CRP2, switched on smooth muscle gene activity in adult cardiac myocytes. *Proc. Natl. Acad. Sci. U. S. A.* **104**:157–162.
- Chi, T. H., et al. 2003. Sequential roles of Brg, the ATPase subunit of BAF chromatin remodeling complexes, in thymocyte development. *Immunity* **19**:169–182.
- Conway, S. J., A. Kruzynska-Frejtag, P. L. Kneer, M. Machnicki, and S. V. Koushik. 2003. What cardiovascular defect does my prenatal mouse mutant have, and why? *Genesis* **35**:1–21.
- de Lange, W. J., C. M. Halabi, A. M. Beyer, and C. D. Sigmund. 2008. Germ line activation of the Tie2 and SMMHC promoters causes noncell-specific deletion of floxed alleles. *Physiol. Genomics* **35**:1–4.
- de la Serna, I. L., Y. Ohkawa, and A. N. Imbalzano. 2006. Chromatin remodeling in mammalian differentiation: lessons from ATP-dependent remodellers. *Nat. Rev. Genet.* **7**:461–473.
- Dick, G. M., et al. 2006. Resistin impairs endothelium-dependent dilation to bradykinin, but not acetylcholine, in the coronary circulation. *Am. J. Physiol. Heart Circ. Physiol.* **291**:H2997–H3002.
- Gallagher, P. J., and B. P. Herring. 1991. The carboxyl terminus of the smooth muscle myosin light chain kinase is expressed as an independent protein, telokin. *J. Biol. Chem.* **266**:23945–23952.
- Gebuhr, T. C. 2003. The role of Brg1, a catalytic subunit of mammalian chromatin-remodeling complexes, in T cell development. *J. Exp. Med.* **198**:1937–1949.
- Griffin, C. T., J. Brennan, and T. Magnuson. 2008. The chromatin-remodeling enzyme BRG1 plays an essential role in primitive erythropoiesis and vascular development. *Development* **135**:493–500.
- Hang, C. T., et al. 2010. Chromatin regulation by Brg1 underlies heart muscle development and disease. *Nature* **466**:62–67.
- Hendricks, K. B., F. Shanahan, and E. Lees. 2004. Role for BRG1 in cell cycle control and tumor suppression. *Mol. Cell. Biol.* **24**:362–376.
- Herring, B. P., G. E. Lyons, A. M. Hoggatt, and P. J. Gallagher. 2001. Telokin expression is restricted to smooth muscle tissues during mouse development. *Am. J. Physiol. Cell Physiol.* **280**:C12–C21.
- Indra, A. K., et al. 2005. Temporally controlled targeted somatic mutagenesis in embryonic surface ectoderm and fetal epidermal keratinocytes unveils two distinct developmental functions of BRG1 in limb morphogenesis and skin barrier formation. *Development* **132**:4533–4544.
- Kang, H., K. Cui, and K. Zhao. 2004. BRG1 controls the activity of the retinoblastoma protein via regulation of p21CIP1/WAF1/SDI. *Mol. Cell. Biol.* **24**:1188–1199.
- Knudson, J. D., et al. 2005. Leptin receptors are expressed in coronary arteries, and hyperleptinemia causes significant coronary endothelial dysfunction. *Am. J. Physiol. Heart Circ. Physiol.* **289**:H48–H56.
- Lu, X., and G. S. Kassab. 2007. Vasoactivity of blood vessels using a novel isovolumic myograph. *Ann. Biomed. Eng.* **35**:356–366.
- Matsumoto, S., et al. 2006. Brg1 is required for murine neural stem cell maintenance and gliogenesis. *Dev. Biol.* **289**:372–383.
- Muchardt, C., and M. Yaniv. 2001. When the SWI/SNF complex remodels...the cell cycle. *Oncogene* **20**:3067–3075.
- Naidu, S. R., I. M. Love, A. N. Imbalzano, S. R. Grossman, and E. J. Androphy. 2009. The SWI/SNF chromatin remodeling subunit BRG1 is a critical regulator of p53 necessary for proliferation of malignant cells. *Oncogene* **28**:2492–2501.
- Ose, T., et al. 2007. Reg I-knockout mice reveal its role in regulation of cell growth that is required in generation and maintenance of the villous structure of small intestine. *Oncogene* **26**:349–359.
- Reyes, J. C., et al. 1998. Altered control of cellular proliferation in the absence of mammalian brahma (SNF2alpha). *EMBO J.* **17**:6979–6991.
- Roberts, C. W., S. A. Galusha, M. E. McMenamin, C. D. Fletcher, and S. H. Orkin. 2000. Haploinsufficiency of Snf5 (integrase interactor 1) predisposes to malignant rhabdoid tumors in mice. *Proc. Natl. Acad. Sci. U. S. A.* **97**:13796–13800.
- Stankunas, K., et al. 2008. Endocardial Brg1 represses ADAMTS1 to maintain the microenvironment for myocardial morphogenesis. *Dev. Cell* **14**:298–311.
- Sumi-Ichinose, C., H. Ichinose, D. Metzger, and P. Chambon. 1997. SNF2beta-BRG1 is essential for the viability of F9 murine embryonal carcinoma cells. *Mol. Cell. Biol.* **17**:5976–5986.
- Touw, K., A. M. Hoggatt, G. Simon, and B. P. Herring. 2007. Hprt-targeted transgenes provide new insights into smooth muscle-restricted promoter activity. *Am. J. Physiol. Cell Physiol.* **292**:C1024–C1032.
- Wang, L., et al. 2005. The BRG1- and hBRM-associated factor BAF57 induces apoptosis by stimulating expression of the cylindromatosis tumor suppressor gene. *Mol. Cell. Biol.* **25**:7953–7965.
- Weaver, T. E., and J. J. Conkright. 2001. Function of surfactant proteins B and C. *Annu. Rev. Physiol.* **63**:555–578.
- Wert, S. E., J. A. Whitsett, and L. M. Noguee. 2009. Genetic disorders of surfactant dysfunction. *Pediatr. Dev. Pathol.* **12**:253–274.
- Xin, H. B., K. Y. Deng, M. Rishniw, G. Ji, and M. I. Kotlikoff. 2002. Smooth muscle expression of Cre recombinase and eGFP in transgenic mice. *Physiol. Genomics* **10**:211–215.
- Zhang, M., H. Fang, J. Zhou, and B. P. Herring. 2007. A novel role of Brg1 in the regulation of SRF/MRTFA-dependent smooth muscle-specific gene expression. *J. Biol. Chem.* **282**:25708–25716.
- Zhou, J., et al. 2009. The SWI/SNF chromatin remodeling complex regulates myocardium-induced smooth muscle-specific gene expression. *Arterioscler. Thromb. Vasc. Biol.* **29**:921–928.